THE UNIVERSITY OF
WARWICK

warwick**publications**wrap

highlight your research

http://wrap.warwick.ac.uk

Magnetic Resonance investigation into the mechanisms involved in the development of high-altitude cerebral edema

Ravjit S Sagoo[1], Charles E Hutchinson[1,2], Alex Wright[3],
Charles Handford[4], Helen Parsons[5], Victoria Sherwood[6],
Sarah Wayte[6], Sanjoy Nagaraja[1], Eddie Ng'Andwe[1],
Mark H Wilson[7] and Christopher HE Imray[2,8,9]; for the
Birmingham Medical Research and Expedition Society

Abstract
Rapid ascent to high altitude commonly results in acute mountain sickness, and on occasion potentially fatal high-altitude cerebral edema. The exact pathophysiological mechanisms behind these syndromes remain to be determined. We report a study in which 12 subjects were exposed to a $FiO_2 = 0.12$ for 22 h and underwent serial magnetic resonance imaging sequences to enable measurement of middle cerebral artery velocity, flow and diameter, and brain parenchymal, cerebrospinal fluid and cerebral venous volumes. Ten subjects completed 22 h and most developed symptoms of acute mountain sickness (mean Lake Louise Score 5.4; $p < 0.001$ vs. baseline). Cerebral oxygen delivery was maintained by an increase in middle cerebral artery velocity and diameter (first 6 h). There appeared to be venocompression at the level of the small, deep cerebral veins (116 cm^3 at 2 h to 97 cm^3 at 22 h; $p < 0.05$). Brain white matter volume increased over the 22-h period (574 ml to 587 ml; $p < 0.001$) and correlated with cumulative Lake Louise scores at 22 h ($p < 0.05$). We conclude that cerebral oxygen delivery was maintained by increased arterial inflow and this preceded the development of cerebral edema. Venous outflow restriction appeared to play a contributory role in the formation of cerebral edema, a novel feature that has not been observed previously.

Keywords
Brain imaging, cerebral blood flow, high altitude, magnetic resonance imaging, physiology

Received 10 August 2015; Revised 8 November 2015; Accepted 27 November 2015

Introduction

On ascent to altitude, there is a reduction in barometric pressure and a consequent fall in the partial pressure of inspired oxygen.[1–3] Acute mountain sickness (AMS) of varying severity can develop in individuals following rapid ascent to high altitudes.[1,4] The symptoms of AMS encompass a wide range of signs and symptoms, the most prominent of which include headache, vomiting, lethargy, and cerebral dysfunction.[1,2] At the extreme end of the spectrum, there is a risk of the potentially fatal high-altitude cerebral edema (HACE) and high-altitude pulmonary edema (HAPE) developing.[5,6]

The brain is particularly sensitive to a lack of oxygen and, therefore, several adaptive mechanisms are believed to occur to maintain adequate oxygen delivery.

[1]Department of Imaging, University Hospitals Coventry and Warwickshire NHS Trust, Coventry, West Midlands, UK
[2]Warwick Medical School, University of Warwick, Coventry, West Midlands, UK
[3]College of Medical and Dental Sciences, University of Birmingham, Birmingham, UK
[4]University Hospitals Birmingham NHS Foundation Trust, Birmingham, UK
[5]Division of Health Sciences, Warwick Medical School, University of Warwick, Coventry, West Midlands, UK
[6]Department of Medical Physics, University Hospitals Coventry and Warwickshire NHS Trust, Coventry, West Midlands, UK
[7]Department of Neurosurgery, Imperial College Healthcare NHS Trust, London, UK
[8]Department of Surgery, University Hospitals Coventry and Warwickshire NHS Trust, Coventry, West Midlands, UK
[9]Coventry University, West Midlands, UK

Corresponding author:
Christopher HE Imray, Department of Surgery, University Hospitals Coventry and Warwickshire NHS Trust, Coventry CV2 2DX, West Midlands, UK.
Email: chrisimray@aim.com

Over a variable time course, hyperventilation, increased heart rate, increased blood pressure, a rise in the hematocrit and hemoglobin are all known to facilitate cerebral oxygen delivery (COD).[7] Specific to the brain, Wilson et al.[8] suggested that both a rise in middle cerebral artery (MCA) diameter and flow velocity are responsible for a rise in cerebral blood flow (CBF) in sustained hypoxia. Until recently, cerebral arterial diameter was widely assumed to stay constant, while cerebral flow velocity was thought to be the sole responsible factor in maintaining cerebral oxygenation.[9]

The exact pathophysiological mechanisms in the development of AMS and HACE have yet to be fully determined. One of the main theories to explain the development of AMS is an increase in intracranial pressure (ICP).[3] Direct ICP measurement is difficult to achieve in healthy volunteers, but the ICP can be inferred indirectly via volume alterations in the different intracranial tissues.[10,11] Hackett et al.[12] have alluded to the development of cerebral edema and its association with AMS in volunteers subjected to sustained hypoxia, particularly within the corpus callosum. Other studies have shown development of cerebral edema, as well as increases in brain parenchymal volume and compensatory decreases in cerebrospinal fluid (CSF) volume in volunteers subjected to sustained hypoxia, but these changes were seen in patients both with and without AMS.[13]

Vasogenic (extracellular water accumulation due to increased permeability of the blood–brain barrier)[12] and cytotoxic (intracellular)[14] edema have been postulated as the mechanisms that underlie HACE. Whether AMS is a milder form of vasogenic and/or cytotoxic, edema remains unclear. However, the rise in parenchymal volume or decrease in CSF volume could also be due to a rise in the CBF and/or efferent restriction of cerebral venous outflow, thus increasing the ICP.[15] In a high-altitude study, Wilson et al.[16] showed that the headache burden was positively related to the retinal vein distension and individuals with relatively narrow transverse sinuses were more prone to hypoxia-induced headaches.

We undertook a sea-level study to observe the effects of normobaric hypoxia in healthy individuals on the brain and cerebral vasculature over a prolonged period of 22 h (AMS and HACE normally take 12–24 h to develop), making multiple assessments to assess the time course of aspects of cerebral perfusion that might be implicated in the development of HACE. We assessed a unification hypothesis of two separate concepts to explain the development of HACE: firstly, the raised arterial inflow (with cytotoxic and vasogenic edema) and, secondly, restricted venous outflow theories.[15] This unification hypothesis was first proposed in schematic format in 2009.[3] Specifically, we aimed to study changes in the cerebral arterial caliber and flow velocity, changes in the small cerebral venous and dural venous sinus caliber, observe the time course of the development of cerebral edema and volume alterations of the brain parenchyma and intracranial CSF. A novel feature of this study was that these variables were measured repeatedly and simultaneously over a 22-h period of sustained hypoxia, which has not been performed previously.

Materials and methods

Subjects and study design

The study design was a prospective observational cohort study, in which subjects were exposed to normobaric hypoxia in a chamber setting. Subjects self-assessed clinical symptoms and various magnetic resonance (MR) sequences were used to assess changes in cerebral parameters. Coventry and Warwickshire NHS Research Ethics Committee provided ethical approval for this study. Written informed consent was obtained from each study participant.

Twelve subjects (10 males, mean age: 26.2 years, range: 21–47 years) were studied over a continuous normobaric hypoxic period of 22 h. None of the subjects had ascended > 1000 m in the preceding six months. Subjects were students interested in wilderness medicine and recruited by word of mouth.

Hypoxia

Subjects were exposed to 22 h of continuous normobaric hypoxia ($FiO_2 = 0.12$, approximately equivalent to an altitude of 4400 m) inside a $2\,m \times 2\,m \times 1.6\,m$ hypoxic tent. Three hypoxic generators were used (Everest Summit Hypoxic Generator, Hypoxic Systems, New York, NY, USA). Build-up of carbon dioxide within the tent was controlled with an air pump (Bair Hugger™, 3 M, Berkshire, UK), which pumped the tent air through a two soda lime scrubber (Spherasorb™ – medical grade soda lime from Intersurgical Ltd UK in canisters by Draeger Medical UK Ltd). The soda lime was replaced at 12 h. Baseline physiological measurements, venous blood samples, and magnetic resonance imaging (MRI) scans were obtained at normoxia ($FiO_2 = 0.21$). Inspired oxygen and carbon dioxide concentrations were checked every 15 min for the first 2 h, every 30 min from 2–10 h, and then every 2 h from 12–22 h. Extended MRI compatible tubing and a tight fitting mask that were connected to one of the three hypoxic generators enabled the subjects to remain hypoxic during the MRI studies. The subjects were scanned at rest and did not undertake exercise during the study period.

Subjects ate and drank ad libitum were kept well hydrated and slept at various points between the 12 and 22-h time points.

Physiological measurements

Physiological measurements were obtained at baseline followed by 2, 4, 6, 11, and 22 h of continuous normobaric hypoxia. Blood pressure was measured using an automated cuff, peripheral arterial oxygen saturation (SaO_2) and heart rate by near infrared finger pulse oximetry probe, and end tidal carbon dioxide ($ETCO_2$) using an infrared capnometer (Dash 3000, GE Medical Systems, Wisconsin, USA).

Whole venous blood samples were obtained at baseline, 11 and 22 h of continuous normobaric hypoxia. Laboratory analysis of hematological (hematocrit and concentration of hemoglobin (Hb), red blood cells, white blood cells, and platelets), biochemical (concentration of sodium, potassium, urea, and creatinine) and inflammatory variables (erythrocyte sedimentation rate (ESR), and concentration of C-reactive protein (CRP)) was carried out on each sample.

Blood oxygen content (BOC) and MCA flow (f) were calculated using equations (1) and (2), respectively.

$$BOC = 1.36 * Hb * SaO_2 \tag{1}$$

$$f = \pi \left(\frac{d}{2}\right)^2 v \tag{2}$$

where d is the MCA diameter and v the MCA flow velocity. The COD was determined using equation (3).

$$COD = BOC * f \tag{3}$$

Headache and Lake Louise scores

The Lake Louise questionnaire and scoring system were used to assess symptoms associated with AMS at baseline and 2, 4, 6, 11, and 22 h of continuous 12% normobaric hypoxia.[17] A total Lake Louise score of >3 including headache at any time point was defined as AMS. Cumulative Lake Louise scores were calculated by adding the Lake Louise scores at each time point to give a total score for each subject.

MRI

Each subject underwent 3-T MRI scanning (GE Signa HDxt, Milwaukee, USA) at baseline, and 2, 4, 6, 11, and 22 h of continuous normobaric 12% hypoxia. The following sequences were obtained:

1. 3D time of flight (TOF) magnetic resonance angiography (MRA) of the circle of Willis was performed to enable measurement of MCA cross-sectional area and diameter (repetition time (TR) = 27 ms; echo time (TE) = 3.4 ms; flip angle (FA) = 20°; matrix = 384 × 256, field of view (FOV) = 210 × 210 mm, slice thickness (ST) = 1.2 mm)

2. A sagittal single-slice 2D electrocardiogram triggered phase-contrast (PC) MRA was performed to enable estimation of the MCA flow velocity (TR = 33 ms; TE = 5.3 ms; FA = 30°; matrix = 256 × 192, FOV = 160 × 160 mm, ST = 5 mm, velocity encoding parameter (VENC) = 150 cm/s). The sagittal slice was centered 1 cm proximal to the bifurcation of the right MCA. The acquisition window was sampled with 25 phases.

3. 3D PC magnetic resonance venography (MRV) of the dural venous sinuses was performed to enable estimation of the volumes of the superior sagittal and transverse venous sinuses (TR = 12 ms; TE = 4 ms; FA = 8°; matrix = 352 × 224, FOV = 240 × 204 mm; acquired ST = 1.6 mm; reconstructed ST = 0.8 mm).

4. T2*-based susceptibility-weighted imaging (SWI) of the whole brain (SWAN® sequence, (susceptibility-weighted angiography) provided by GE Healthcare, Buckinghamshire, UK) was performed to assess changes in the deep cerebral venous anatomy (TR = 42 ms; TE = 24.7 ms; FA = 15°; matrix = 320 × 224, FOV = 220 × 200 mm; acquired ST = 2.6 mm; reconstructed ST = 1.3 mm).

5. Diffusion-weighted images of the whole brain (TR = 10,000 ms; TE = 95 ms; matrix = 256 × 256; FOV = 240 × 240 mm; ST = 4.0 mm; b = 0, 800, 1000) were acquired at each time point, from which apparent diffusion coefficient (ADC) maps were calculated to assess for edema.

6. T1-based 3D fast spoiled gradient echo imaging (FSPGR) of the whole brain was performed to enable estimation of brain and CSF volume (TR = 7.8 ms; TE = 3 ms; FA = 12°; matrix = 256 × 256; FOV = 220 × 165 mm; acquired ST = 2.6 mm; reconstructed ST = 1.3 mm).

Image analysis

The 3D TOF MRA data were imported into a GE Advantage Workstation 4.6 (GE Healthcare, Buckinghamshire, UK) to estimate the MCA diameter and cross-sectional area. Three raters who were blinded to the subject and time point at which the scan had been acquired, undertook the measurements independently. The M1 segment of the MCA was identified bilaterally using the orthogonal multiplanar reconstruction (MPR) module and each MCA M1 segment was manually divided into five equally spaced data points. The cross-sectional view, the maximal diameter and cross-sectional area were manually measured at each data point in bilateral MCA M1 segments. A mean value

for the MCA diameter and cross-sectional area at each time point was calculated from the 10 data points.

The 2D PC-MRA data were also imported into the GE Advantage Workstation 4.6. MCA flow velocities were obtained using the flow analysis module. The MCA margins were defined automatically and adjusted manually for each phase if necessary. Mean and peak systolic flow velocities were determined automatically by the flow analysis module.

Analyze 11.0 (AnalyzeDirect, KS, USA) was used to calculate the total volumes of the superior sagittal and transverse venous sinuses using the 3D PC-MRV data acquired at each time point. The semi-automatic threshold technique (using standardized minimum and maximum threshold values) was used to define and extract the appropriate venous sinuses to enable automated volume calculation.

The deep venous space was calculated in by quantifying the total volume of all voxels corresponding with deep veins within the brain tissue, which have low signal intensity on SWI. SWI were segmented to remove the skull and CSF using SPM8 (Wellcome Trust Centre for Neuroimaging, University College, London, UK). Using a Matlab (Mathworks Inc., Cambridge, UK) program written in-house, a linear intensity normalization of the voxel data was performed to correct for global intensity variations between time points. Voxels falling within a user defined intensity window (Figure 1) were summed and used to calculate the deep venous space based on the voxel dimensions. The 2-h time point was used as a baseline for these measurements due to an expected
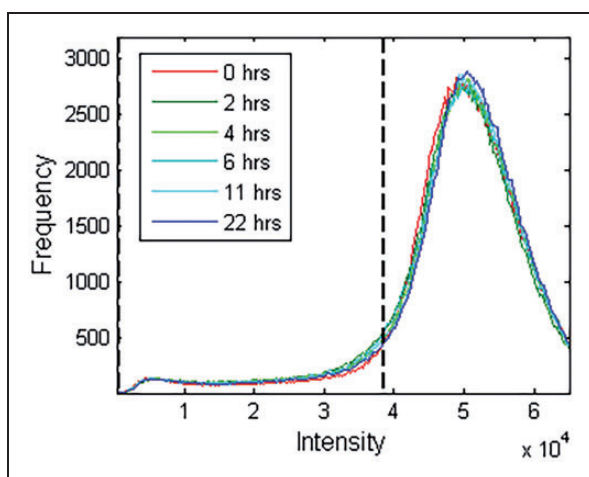

Figure 1. A histogram demonstrating voxel intensities for the whole brain for all subjects at the specific time points. The number of voxels falling below the vertical dashed line (the set threshold level) was calculated to enable venous space quantification.

increase from baseline to 2 h caused by the magnetic susceptibility of deoxyhemoglobin (the BOLD effect).

ADC maps were calculated after importing the diffusion-weighted images into the GE Advantage Workstation 4.6. Circular regions of interest (ROI) of $1 \, cm^2$ were placed bilaterally within the frontal white matter, lentiform nuclei (gray matter), occipital white matter, cerebellar white matter, and the genu and splenium of the corpus callosum. The mean ADC value within each right and left circular ROI was then calculated. The right and left ADC values for a given anatomical region were averaged to give a single mean ADC value for the region.

The T1-weighted 3D FSPGR data were imported into the FMRIB Software Library (FSL) 5.0 (FMRIB Group, Oxford, UK) to quantify brain parenchymal and CSF volumes. Initially, the Brain Extraction Tool (BET) was used to delete all non-brain tissue. The FMRIB's Automated Segmentation Tool (FAST) was then used to segment the brain image into different tissue types (gray matter, white matter, and CSF). This tool also automatically corrects for any spatial intensity variations. Tissue volume quantification was carried out using the FSLSTATS command for each of the segmented tissue images at each time point.

Statistical analysis

Analysis of repeated observations was performed using the linear mixed models procedure in SPSS v22 (IBM, NY, USA) to examine the effects of time exposed to hypoxia on each dependent variable. The linear mixed models procedure does not require a balanced design so is able to account for all missing data. Model parameters were estimated using the restricted maximum likelihood method and covariance was modeled as unstructured. Sidak's adjustment for multiple pairwise comparisons and paired t-tests were employed as appropriate. Study size was in part determined by power calculations but also based upon similar studies. To assess the relationship of selected variables, bivariate correlations for ordinal data (Spearman's Rho) and continuous data (Pearson's correlation) were used as appropriate. Statistical significance was set at $p \leq 0.05$.

Results

Two of the 12 subjects were unable to complete the study due to severe AMS and had to be withdrawn after the 11-h time point. The data set was otherwise complete. Changes in the basic physiological variables with time exposed to normobaric hypoxia are displayed in Table 1, and Table 2 presents changes in the measured radiological variables at each time point. Both tables summarize the estimated marginal means of the

Table 1. Estimated marginal means, significance of change, and 95% CIs for each measured physiological variable and total Lake Louise and headache scores using multilevel modeling.

	0 h (normoxia)	2 h hypoxia	4 h hypoxia	6 h hypoxia	11 h hypoxia	22 h hypoxia	Sig
Fraction of inspired oxygen	0.21	0.12	0.12	0.12	0.12	0.12	<0.05
Fraction of inspired carbon dioxide	0.03	0.23	0.26	0.25	0.23	0.27	<0.05
Peripheral oxygen saturation, %	99.33 (98.19–99.75)	82.92 (78.90–86.93)	82.92 (80.95–84.88)	84.17 (80.81–87.53)	83.83 (79.99–87.67)	84.98 (82.77–87.19)	<0.001
End tidal CO_2, %	5.36 (5.09–5.63)	1.75 (1.24–2.27)	2.21 (1.87–2.55)	1.92 (1.57–2.27)	2.13 (1.70–2.56)	1.88 (1.43–2.33)	<0.001
Heart rate, beats/min	64.92 (60.49–69.35)	71.50 (64.24–78.76)	80.50 (74.49–86.51)	78.25 (72.24–84.26)	76.92 (67.95–85.89)	85.69 (80.45–90.93)	<0.001
Systolic blood pressure, mmHg	123.33 (118.02–128.65)	126.42 (118.92–133.92)	121.83 (115.25–28.42)	127.92 (122.48–133.35)	133.67 (126.89–140.44)	130.72 (122.84–138.60)	0.085
Diastolic blood pressure, mmHg	73.58 (65.45–81.72)	68.92 (62.26–75.58)	71.50 (66.85–76.15)	71.08 (63.89–78.28)	76.83 (70.34–83.32)	76.05 (68.45–83.65)	0.068
Total Lake Louise score	0	1.33 (0.77–1.90)	1.33 (.71–1.96)	2.00 (0.67–3.33)	2.75 (1.70–3.80)	5.40 (3.19–7.62)	0.004
Headache score	0	0	0.30 (0–0.50)	0.60 (0.10–1.10)	1.40 (0.80–2.00)	1.60 (1.00–2.20)	<0.001
Hemoglobin concentration, g/dL	15.09 (14.62–15.56)		15.26 (14.68–15.85)		15.26 (14.68–15.85)	15.44 (14.63–16.25)	0.445
Platelet count, $\times 10^9$/L	236.5 (208.28–264.71)				239.96 (215.29–264.63)	234.56 (216.91–252.21)	0.389
Red blood cell count, $\times 10^{12}$/L	5.03 (4.88–5.18)				5.09 (4.94–5.24)	5.12 (4.85–5.39)	0.404
Hematocrit	0.44 (0.43–0.46)				0.44 (0.43–0.46)	0.45 (0.43–0.47)	0.623
Serum sodium concentration, mmol/L	143.49 (142.45–144.52)				141.93 (140.8–143.06)	142.3 (141.33–143.27)	0.09
Serum potassium concentration, mmol/L	4.53 (4.32–4.73)				4.29 (4.05–4.54)	4.63 (4.38–4.89)	0.186
Serum urea concentration, mmol/L	5.73 (4.86–6.61)				5.64 (4.71–6.57)	5.67 (5.02–6.33)	0.906
Serum creatinine concentration, μmol/L	78.81 (70.85–85.48)				81.4 (72.83–90.5)	83.6 (73.76–90.58)	0.07

CI: confidence intervals.

Table 2. Estimated marginal means, significance of change, and 95% CIs for each measured radiological variable using multilevel modeling.

	0 h (normoxia)	2 h hypoxia	4 h hypoxia	6 h hypoxia	11 h hypoxia	22 h hypoxia	Sig
MCA diameter, mm	3.10 (2.89–3.30)	3.19 (3.00–3.38)	3.18 (2.97–3.40)	3.23 (3.00–3.44)	3.12 (2.91–3.33)	3.23 (3.02–3.43)	0.065
MCA area, mm^2	9.35 (8.18–10.52)	9.89 (8.693–11.08)	9.84 (8.58–11.10)	10.08 (8.69–11.47)	9.39 (8.19–10.59)	10.02 (8.81–11.23)	0.34
MCA peak systolic flow velocity, cm/s	70.41 (55.92–84.90)	82.21 (63.34–101.08)	90.68 (70.54–110.82)	84.93 (63.19–106.66)	83.91 (62.08–105.74)	78.77 (59.54–98.01)	0.197
MCA mean flow velocity, cm/s	47.53 (39.69–55.36)	57.09 (45.92–68.27)	53.83 (42.81–64.86)	55.46 (43.71–67.21)	55.88 (42.81–68.95)	53.44 (43.15–63.72)	0.05
MCA peak systolic flow, ml/s	6.58 (5.01–8.14)	7.98 (6.08–9.88)	8.67 (6.95–10.40)	8.36 (6.43–10.29)	7.767 (5.68–9.85)	8.00 (5.67–10.32)	0.101
MCA mean flow, ml/s	4.49 (3.49–5.49)	5.49 (4.49–6.49)	5.14 (4.27–6.02)	5.44 (4.47–6.42)	5.15 (3.95–6.36)	4.82 (3.88–5.75)	0.292
Blood oxygen content, ml O$_2$/dL blood	20.20 (19.50–20.90)	16.88 (15.79–17.96)	16.86 (16.18–17.55)	17.14 (16.08–18.2)	17.50 (16.40–18.60)	18.15 (17.31–18.98)	<0.001
Oxygen delivery, ml/s	9.07 (7.09–11.05)	9.25 (7.47–11.03)	8.70 (7.13–10.28)	9.37 (7.42–11.33)	8.91 (6.90–10.93)	11.12 (7.63–14.61)	0.294
Whole brain ADC values, × 10-4/mm^3 ADC values, × 10-4/mm^3	8.90 (8.64–9.15)	9.08 (8.75–9.41)	9.13 (8.88–9.38)	9.14 (8.98–9.31)	9.19 (8.94–9.44)	9.40 (9.20–9.60)	<0.001
ACA territory ADC (Frontal) values, × 10-4/mm^3 (R & L Mean)	5.38 (4.91–5.85)	5.70 (5.20–6.20)	5.75 (5.37–6.13)	5.62 (5.23–6.01)	5.64 (5.16–6.13)	5.69 (5.24–6.15)	0.12
MCA territory (LN) ADC values, × 10-4/mm^3 (R & L Mean)	6.87 (6.50–7.23)	7.15 (6.86–7.43)	7.03 (6.69–7.37)	7.21 (6.77–7.65)	7.04 (6.70–7.37)	7.18 (6.79–7.58)	0.157
PCA territory (Occipital) ADC values, × 10-4/mm^3 (R & L Mean)	6.19 (5.58–6.79)	6.17 (5.38–6.97)	6.20 (5.46–6.94)	6.32 (5.72–6.92)	6.25 (5.56–6.93)	6.47 (5.88–7.05)	0.061
Cerebellar ADC values, × 10-4/mm^3 (R & L Mean)	7.44 (7.13–7.75)	7.46 (7.17–7.76)	7.45 (7.03–7.86)	7.43 (7.12–7.73)	7.42 (7.17–7.66)	7.60 (7.34–7.87)	0.761
Corpus callosum (Genu) ADC values, × 10-4/mm^3 (R & L Mean)	16.90 (15.96–17.85)	17.22 (16.32–18.13)	17.41 (16.66–18.16)	17.54 (16.70–18.39)	17.08 (16.02–18.14)	18.25 (17.40–19.10)	<0.001
Corpus callosum (Splenium) ADC Values, × 10-4/mm^3	20.31 (19.30–21.31)	20.62 (19.50–21.75)	21.05 (19.87–22.23)	20.71 (19.73–21.69)	22.17 (21.11–23.24)	21.89 (20.78–22.99)	<0.001
Intracranial CSF volume, ml	283.72 (263.31–304.12)	278.99 (252.30–305.68)	282.58 (253.78–311.28)	281.49 (256.74–306.25)	276.90 (251.84–301.96)	269.61 (248.14–291.08)	0.005
Gray matter volume, ml	679.02 (636.63–721.40)	694.46 (648.94–739.98)	685.89 (646.81–724.97)	691.88 (652.89–738.86)	687.37 (647.48–727.27)	695.32 (651.11–739.52)	0.002
White matter volume, ml	573.90 (534.17–613.62)	574.24 (531.58–616.89)	577.45 (534.18–620.71)	575.11 (534.54–615.67)	579.35 (535.07–623.63)	586.76 (544.75–628.77)	<0.001
Total brain parenchymal volume, ml	1252.91 (1175.94–1329.88)	1268.69 (1184.37–1353.01)	1263.34 (1187.22–1339.46)	1270.99 (1190.38–1351.59)	1266.73 (1190.92–1342.54)	1282.07 (1201.49–1362.65)	0.002
Superior sagittal and transverse sinus volume, ml	10.51 (0.07–11.94)	10.90 (9.11–12.68)	10.39 (9.00–11.78)	10.23 (8.87–11.59)	10.21 (8.93–11.48)	10.21 (8.67–11.75)	0.692
Deep cerebral venous volume, ml	115.91 (106.77–125.05)	115.91 (106.77–125.05)	106.74 (99.00–114.48)	110.16 (98.71–121.62)	105.21 (94.54–115.88)	97.34 (88.84–108.43)	0.003

CSF: cerebrospinal fluid; ADC: apparent diffusion coefficient; ACA: anterior cerebral artery; MCA: middle cerebral artery; PCA: posterior cerebral artery; CI: confidence intervals.

measured variables, confidence intervals, and the significance of change at each time point.

Ten of the 12 subjects (including the two who left the study early) developed a total Lake Louise score of 3 or more at any individual time point (i.e. had a diagnosis of AMS). The mean total Lake Louise and headache scores for all subjects were seen to rise steadily at each time point, with the largest increase at 22 h.

SpO_2 and $ETCO_2$ significantly decreased at all hypoxic time points compared to baseline, whereas the heart rate rose significantly at all-time points compared to baseline ($p < 0.001$ for each of the three variables). The systolic and diastolic blood pressures appeared to steadily rise, although this trend was not statistically significant ($p = 0.085$ and 0.068, respectively). No significant changes in any of the venous blood components were seen.

The mean MCA flow velocity increased and peaked after 2 h of continuous hypoxia exposure (47.53 to 57.09 cm/s; $p = 0.05$) before falling towards baseline values for the remainder of the study. The MCA diameter displayed a similar trend of an early rise before decreasing, although this was not statistically significant ($p = 0.065$). The calculated mean flow through the MCA did not increase or decrease significantly over the 22-h course of the study when analyzed using the linear mixed models procedure. However, performing paired t-test analyses showed that the mean MCA flow rose significantly from 4.5 to 6.1 ml/s ($p < 0.05$) between the baseline and 2 h before falling towards baseline values. The calculated BOC was consistently low at all-time points compared to the normoxic, baseline levels ($p < 0.001$). Calculated COD did not change significantly throughout the hypoxic period.

The superior sagittal and transverse venous sinus volumes did not change significantly in response to the prolonged hypoxic challenge. However, by 22 h, there appeared to be an element of venocompression at the level of the small, deep cerebral veins (116 cm^3 at 2 h to 97 cm^3 at 22 h; $p < 0.05$).

A late increase in total brain parenchymal volume was seen at 22 h compared to baseline (1253 ml at baseline to 1282 ml at 22 h; $p < 0.05$). Increases in both gray matter (679 ml at baseline to 695 ml at 22 h; $p < 0.05$) and white matter (574 ml at baseline to 585 ml at 22 h; $p < 0.001$) volumes contributed to the overall brain parenchymal volume increase. A compensatory significant decrease in total intracranial CSF was seen at 22 h compared to baseline (284 ml to 270 ml; $p < 0.05$). In addition, the increase in total brain parenchymal volume correlated strongly with the decrease in CSF volume between 0 and 22 h (Pearson $= -0.67$, $p < 0.05$) (Figure 2). Strong correlation was seen between the increase in white matter volume at 22 h

and the cumulative Lake Louise score for each patient at 22 h (Spearman rho $= 0.65$, $p < 0.05$) (Figure 3). No significant correlation was observed between any other variable and the headache or Lake Louise score.

Taking into account all the ADC ROIs at each time point, a significant rise in the mean whole brain ADC value was observed after exposure to 11 and 22 h of hypoxia (8.9×10^{-4} to 9.2×10^{-4} and 9.4×10^{-4} mm^2/s, respectively; $p < 0.001$). With each regional ROI analyzed separately, there were significant rises compared to baseline in the ADC value within the genu (16.9×10^{-4} at baseline to 18.3×10^{-4} mm^2/s at 22 h; $p < 0.001$) and the splenium (20.3×10^{-4} at baseline to 22.8×10^{-4} at 11 and 21.9×10^{-4} mm^2/s at 22 h; $p < 0.001$). The rest of the ROIs did not display any significant increases or decreases in ADC value over time, although there was an upward trend within the occipital lobes (6.19×10^{-4} at baseline to 6.47×10^{-4} mm^2/s; $p = 0.06$).

Discussion

The novel feature of this study is that arterial inflow, large and small vessel venous outflow, cerebral edema (ADC), brain parenchymal volumes, and intracranial CSF volumes have been measured repeatedly and simultaneously over a 22-h period of sustained hypoxia. As a consequence, this study gives insights into the time course of both the adaptive processes as well as some of the potentially maladaptive processes on acute exposure to a $FiO_2 = 0.12$ (which is equivalent to approximately 4400 m). This is one of the first studies to use 3 T MRI scanning for more than 10 h and this is important as many of the more severe high-altitude syndromes develop over a longer period of time – classically after a night at the new altitude.

This combination of time (including overnight) and simulated altitude represents the sort of stimulus that would be expected to cause a significant level of acute high-altitude illness and this was found to be the case with most of the subjects. Ten of the 12 subjects developed a total Lake Louise score of more than 3 (in keeping with a diagnosis of 'AMS'). The mean total Lake Louise and headache scores for all subjects were seen to rise steadily at each time point, with the largest increase at 22 h. COD was maintained by increases in MCA velocity and there is emerging evidence that there is also an associated increase in MCA diameter.[8,18,19] This is the first time that COD has been shown to be maintained to 22 h when assessed by MR.

Late rises in ADC values within the genu and splenium of the corpus callosum confirm the build-up of regional water content and are an indirect measure of cerebral edema. This supports the findings observed by Hackett et al.[12] We found the observed increase in
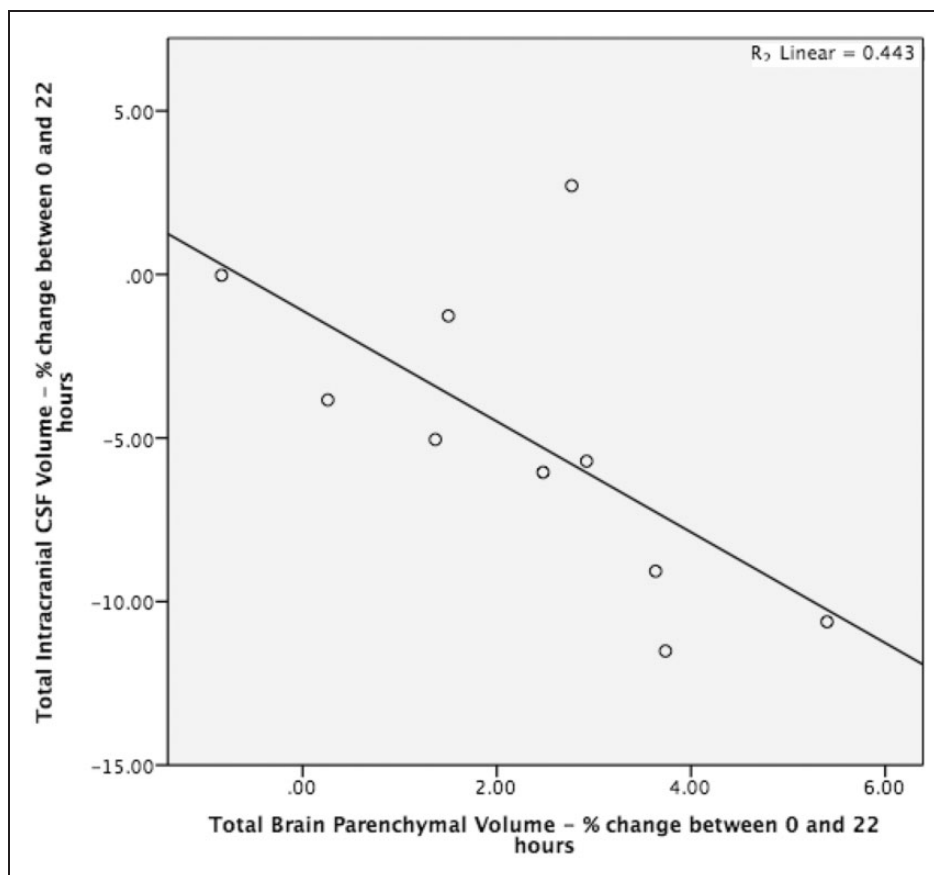
Figure 2. A graph demonstrating the correlation between the percentage change of the total intracranial CSF volume and the total brain parenchymal volume over the 22-h study period.

brain parenchymal volumes at 22 h was associated with decreased brain CSF volumes (confirming "internal validation" of our methodology of independently measuring the segmented CSF and brain parenchymal volumes) and also a reduction in small venous vessel volumes (SWI sequence) at 22 h, further increasing the Starling pressure driving edema formation. A decreased ability to buffer these parenchymal brain volume changes will be reflected by rises in ICP and eventually HACE.[3] Interestingly, a correlation was found between the cumulative Lake Louise score and an increase in brain white matter volume at 22 h. This study supports certain aspects of the recent Lawley et al.[20] publication where they found an increase in brain volume (predominantly in the gray matter) at 10 h, with an associated fall in the cerebral component of CSF. They also found a statistically significant relationship between change in ICP (measured non-invasively by MRI) and AMS severity ($R^2 = 0.71$, $B = 2.3$, $p < 0.01$) after 10 h. We studied our subjects for a further 12 h and found, as would be predicted, higher levels of AMS symptoms. In addition, we found a later increase in total brain parenchymal volume (gray and white matter) at 22 h compared to baseline.

This study has shown for the first time a possible mechanistic link between hypoxia, increased arterial inflow, a hypothesized rise in Starling pressures, and the subsequent development of parenchyma brain edema and the clinical development of AMS. We, therefore, propose a unification hypothesis, which involves the activation of train of etiologic factors progressing from cerebral arterial to venous to parenchymal compartments, and also a clear staged time course (Figure 4):

1. Firstly, hypoxia results in increased CBF (in order to maintain COD).[8]
2. The increased arterial inflow is associated with an increase in venous outflow. The increase in venous outflow requires increased "driving pressures" to maintain CBF (raised arterial pressures).[21]
3. The venous outflow restriction or resistance could take place at a number of levels (Figure 5):
   a. Intracerebral as appears to be the case in this study, which has not been demonstrated previously.
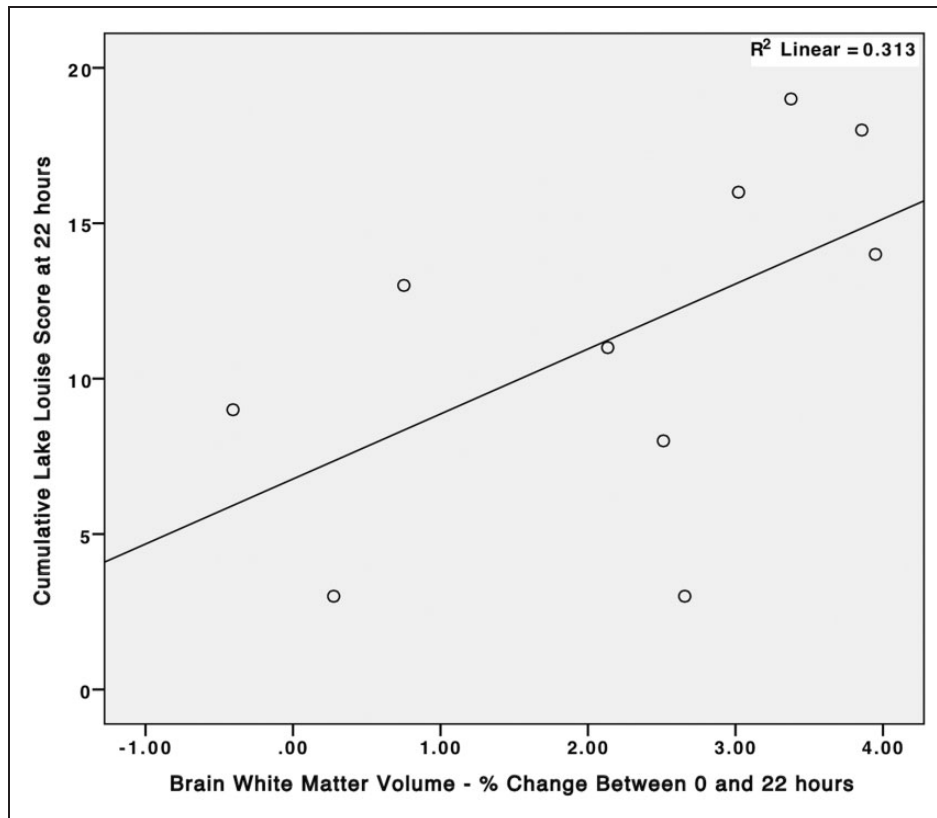   b. Intracranial (in the great veins and dural venous sinuses).[16]

Figure 3. A graph demonstrating the correlation between the percentage volume change of the brain white matter and the cumulative Lake Louise score at 22 h.

c. Extracranially (elevated CVP, anatomic venous restrictions).[3,22]

The required increase in "driving pressure" will in turn perturbate "Starling pressures" and is likely to be a contributing factor in the formation of parenchymal edema. As edema develops, there will be further restriction in venous outflow and this could result in a dangerous positive feedback loop. Reduction of the cerebral capacitance will eventually occur resulting in an increase in ICP and, ultimately, AMS/HACE. The increased CBF will increase the likelihood of vasogenic edema[3,19] and localized cellular hypoxia makes cells susceptible to cytotoxic edema.[23,24] It should be noted that in this study the "venous outflow restriction" appears to be associated with smaller venous vessels rather than the large vessels / anatomical variants described by Wilson et al.[16] (who found that restriction in transverse venous sinus outflow was associated with more headaches and proximal venous distension between 90 and 180 min of exposure to 12% oxygen). The observed decreasing trend for transverse venous sinus volumes in the current study was modest without

reaching significance and, therefore, could be attributed to a small study sample.

The experimental design using a hypoxic tent adjacent to the MRI room functioned well. Subjects were comfortable, were kept well hydrated and in constant communication with the investigators throughout the time of exposure to hypoxia. Care was taken to maintain hypoxia while transferring from the tent to the scanner and during the period of the scan.

Study limitations

Limitations of this study include a small but stable accumulation of carbon dioxide in the tent, despite soda lime scrubbers, which may have contributed to the increase in peak systolic flow velocity in the MCA. However, during scanning, re-breathing was not an issue and there were low $ETCO_2$ readings. There were a relatively small number of subjects for investigation of a variable condition such as AMS with symptoms usually occurring 6–12 h after arrival at high altitude. However, peak symptoms would be expected to occur somewhat later after 24 h exposure. Nevertheless, two subjects were withdrawn after 11 h of
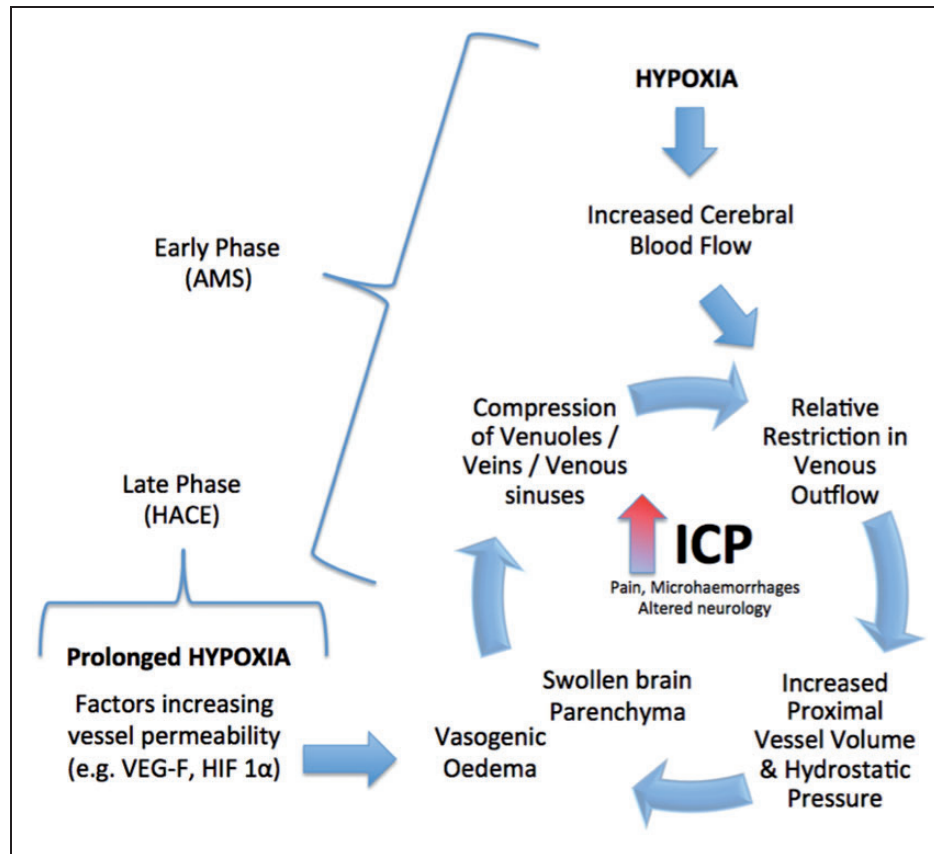
Figure 4. A diagram illustrating the proposed sequence of events thought to contribute towards the development of AMS. Source: Wilson MH and Imray CHE. The cerebral venous system and hypoxia. J Appl Physiol.Epub ahead of print 20 August 2015.DOI: 10.1152/japplphysiol.00327.2015.

hypoxia and significant symptoms occurred in the remainder. As the subjects were all young, results cannot necessarily be extrapolated to older people. In most reports, young subjects are more prone to develop AMS.[25] One theory that older people with more age-related atrophy might tolerate cerebral swelling better has been suggested.

Wider clinical relevance

The results of this study may have important translational implications.[26] ICP is the primary neurological parameter that guides therapy on neurointensive care. Understanding the cerebrovascular interactions that effect ICP is vital in the management of both trauma and stroke patients. The optimization of cerebral perfusion pressure (CPP) is determined by ICP (CPP = Mean Arterial Pressure – ICP). Intracranial venous outflow pressure closely correlates with ICP.[27]

The effects of carbon dioxide and hyperventilation on CBF are well known.[28] The effects of hypoxia, and in particular the changes that occur over a period of time, may aid the understanding of the interplay between chest and intracranial physiology. Hypoxia, for example secondary to chest sepsis or adult respiratory distress syndrome is common in the neurocritical patient.[29] As such, the management of cerebral oxygenation, as well as carbon dioxide are integral to good neurocritical care and is likely to be crucial to optimizing the correct therapeutic regime.

In this study, hypoxia resulted in parenchymal brain swelling. Subsequent development of cerebral edema was found, which would eventually result in a rise in ICP. This was attributed to compression of the cerebral venous system, restricting venous outflow, and possibly a Starling resistor mechanism.[30] In an animal model, venous hypertension has been associated with increases in brain volume and this was caused by vessel dilation. Cerebral edema only occurred if there was also associated cerebral tissue injury.[31] Acute hypoxia can cause tissue injury through a number of different mechanisms such as direct damage to basal membrane structures,[32] VEGF,[24] or free radicals.[25]

Interestingly, there is corroborative clinical evidence. It has been shown in a study of sub-arachnoid hemorrhage (SAH) patients that increased ICP values
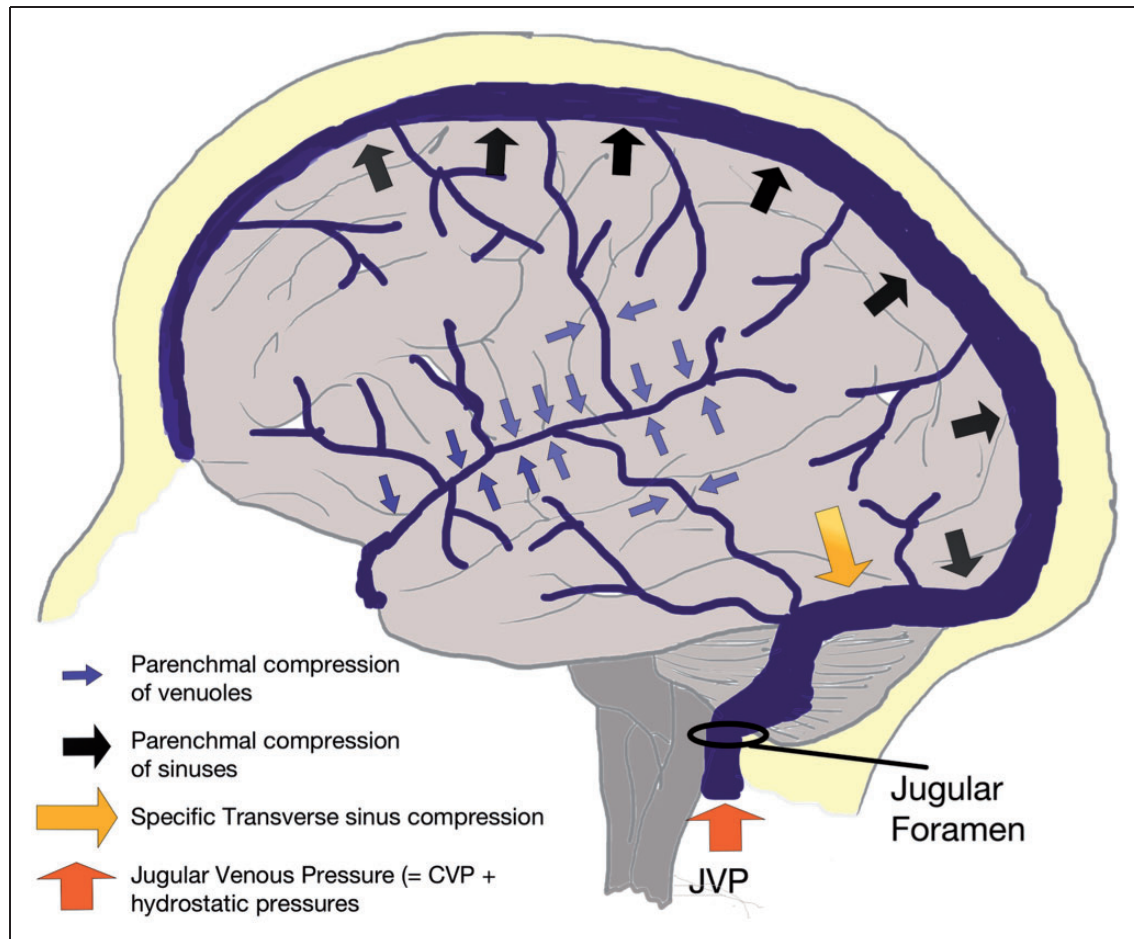
Figure 5. A diagram illustrating the intracranial and extracranial sources thought to contribute to venous outflow restriction. Source: Wilson MH and Imray CHE. The cerebral venous system and hypoxia. *J Appl Physiol.*Epub ahead of print 20 August 2015. DOI: 10.1152/japplphysiol.00327.2015.

correlated with increased venous flow velocities and were associated with poor outcome.[33] Flow velocity of the transversal sinus was thought to be a highly sensitive, reliable, and early predictor of outcome in SAH. An explanation is that raised ICP would reduce intracerebral venous diameters and in turn, if CBF were to be maintained, a rise in venous velocities would be expected and this would result in changes in the Starling pressures at the capillary level.

Conclusions

In conclusion, this 22-h study has used a variety of MR imaging techniques to document the development of HACE in normal individuals. There was an early increase in CBF which maintained COD. Mild clinical symptoms appeared after a few hours and these gradually increased in severity over time. Cerebral edema developed later and this occurred in conjunction with an increase in the brain parenchyma volumes and a reduction in CSF volumes. Inability to buffer this

brain swelling would result in rises in ICP and this is likely to be associated with deterioration in the patient's condition. A possible novel mechanism involving local edema causing a reduction in post capillary venous diameters has been observed. In order to maintain the high CBF through smaller vessels, there must be alterations in the Starling pressures, and these could be one of the causative factors, in parallel with reduced cerebral buffering, in the development of life threatening raised intracerebral pressures seen in HACE. The same mechanism may be implicated in raised ICP from other causes.

Declaration of conflicting interests

The author(s) declared no potential conflicts of interest with respect to the research, authorship, and/or publication of this article.

Authors' contributions

CI, AW, CEH, SW, MW, and RS contributed to study design. SW was involved in producing the parameters for the various MR sequences. EN performed the MR scanning for all subjects. CI, AW, and CH participated in clinical/physiological data collection and analysis. RS, CEH, VS, SW, and SN contributed to radiological data collection and analysis. HP and RS performed the statistical analysis. RS, CI, and AW did the literature review and wrote the manuscript. All authors critically reviewed the final draft of the manuscript and have given approval for the version submitted.

References

1. Hackett PH and Roach RC. Current concepts: high altitude illness – a practical review. *N Engl J Med* 2001; 345: 107–114.
2. Hackett PH and Roach RC. High-altitude medicine. In: Auerbach PA (ed.) *Wilderness medicine* 2000. St Louis: Mosby, pp.1–37.
3. Wilson MH, Newman S and Imray CH. The cerebral effects of ascent to high altitudes. *Lancet Neurol* 2009; 8: 175–191.
4. Imray C, Booth A, Wright A, et al. Acute altitude illnesses. *BMJ* 2011; 343: d4943.
5. Hultgren HN, Spickard WB, Hellriegel K, et al. High altitude pulmonary edema. *Medicine* 1961; 40: 289–313.
6. Hackett PH and Roach RC. High altitude cerebral edema. *High Alt Med Biol* 2004; 5: 136–146.
7. Ward M, Milledge JS and West JB. *High altitude physiology*, 3rd ed. London: Arnold Publishers, 2000.
8. Wilson MH, Edsell ME, Davagnanam I, et al. Cerebral artery dilatation maintains cerebral oxygenation at extreme altitude and in acute hypoxia – an ultrasound and MRI study. *J Cereb Blood Flow Metab* 2011; 31: 2019–2029.
9. Giller CA. The emperor has no clothes: velocity, flow, and the use of TCD. *J Neuroimaging* 2003; 13: 97–98.
10. Wilson MH and Milledge J. Direct measurement of intracranial pressure at high altitude and correlation of ventricular size with acute mountain sickness. *Neurosurgery* 2008; 63: 970–974.
11. Wright AD, Imray CHE, Morrissey MSC, et al. Intracranial pressure at high altitude and acute mountain sickness. *Clin Sci* 1995; 89: 201–204.
12. Hackett PH, Yarnell PR, Hill R, et al. High-altitude cerebral edema evaluated with magnetic resonance imaging: clinical correlation and pathophysiology. *JAMA* 1998; 280: 1920–1925.
13. Kallenberg K, Bailey DM, Christ S, et al. Magnetic resonance imaging evidence of cytotoxic cerebral edema in acute mountain sickness. *J Cereb Blood Flow Metab* 2007; 27: 1064–1071.
14. Houston CS and Dickinson J. Cerebral form of high-altitude illness. *Lancet* 1975; 2: 758–761.
15. Wilson MH, Imray CHE and Hargens AR. The headache of high altitude and microgravity – similarities with clinical syndromes of cerebral venous hypertension. *High Alt Med Biol* 2011; 12: 379–386.
16. Wilson MH, Davagnanam I, Holland G, et al. Cerebral venous system and anatomical predisposition to high-altitude headache. *Ann Neurol* 2013; 73: 381–389.
17. Roach RC, Bartsch P, Hackett PH, Oelz O. The Lake Louise AMS Scoring Consensus Committee. The Lake Louise acute mountain sickness scoring system. In: Sutton JR, Coates G and Huston CS (eds) *Hypoxia and molecular medicine: proceedings of the 8th international hypoxia symposium*, Lake Louise, Alberta, Canada, 9–13 February 1993, pp. 272–274. Burlington, VT: Queen City Printers.
18. Ogoh S, Sato K, Nakahara H, et al. Effect of acute hypoxia on blood flow in vertebral and internal carotid arteries. *Exp Physiol* 2013; 98: 692–698.
19. Imray C, Chan C, Stubbings A, et al. Time course variations in the mechanisms by which cerebral oxygen delivery is maintained on exposure to hypoxia/altitude. *High Alt Med Biol* 2014; 15: 21–27.
20. Lawley JS, Alperin N, Bagci AM, et al. Normobaric hypoxia and symptoms of acute mountain sickness: elevated brain volume and intracranial hypertension. *Ann Neurol* 2014; 75: 890–898.
21. Imray CHE, Myers SD, Pattinson KTS, et al. Effects of exercise on cerebral perfusion in humans at high altitude. *J Appl Physiol* 2005; 99: 699–706.
22. Willmann G, Fischer MD, Schommer K, et al. Missing correlation of retinal vessel diameter with high-altitude headache. *Ann Clin Transl Neurol* 2014; 1: 59–63.
23. Dorward DA, Thompson AA, Baillie JK, et al. Change in plasma vascular endothelial growth factor during onset and recovery from acute mountain sickness. *Respir Med* 2007; 101: 587–594.
24. Bailey DM, Kleger GR, Holzgraefe M, et al. Pathophysiological significance of peroxidative stress, neuronaldamage, and membrane permeability in acute mountain sickness. *J Appl Physiol* 2004; 96: 1459–1463.
25. McDevitt M, McIntosh SE, Rodway G, et al. Risk determinants of acute mountain sickness in trekkers in the Nepali Himalaya: a 24-year follow-up. *Wilderness Environ Med* 2014; 25: 152–159.
26. Imray CHE, Grocott MPW, Wilson MH, Hughes A, Auerbach PS. Extreme, expedition and wilderness medicine. *The Lancet* 2015; 386(10012): 2520–2525.
27. Johnston IH and Rowan JO. Raised intracranial pressure and cerebral blood flow. 3. Venous outflow tract pressures and vascular resistances in experimental intracranial hypertension. *J Neurol Neurosurg Psychiatry* 1974; 37: 392–402.
28. Coles JP, Minhas PS, Fryer TD, et al. Effect of hyperventilation on cerebral blood flow in traumatic head injury: clinical relevance and monitoring correlates. *Crit Care Med* 2002; 30: 1950–1959.
29. Lee K and Rincon F. Pulmonary complications in patients with severe brain injury. *Crit Care Res Pract* 2012; 2012: 8.
30. Simard JM, Kent TA, Chen M, et al. Brain oedema in focal ischaemia: molecular pathophysiology and theoretical implications. *Lancet Neurol* 2007; 6: 258–268.
31. Cuypers J, Matakas F and Potolicchio SJ. Effect of central venous pressure on brain tissue pressure and brain volume. *J Neurosurg* 1976; 45: 89–94.

32. Miserocchi G, Passi A, Negrini D, et al. Pulmonary interstitial pressure and tissue matrix structure in acute hypoxia. *Am J Physiol Lung Cell Mol Physiol* 2001; 280: L881–L887.

33. Niesen WD, Rosenkranz M, Schummer W, et al. Cerebral venous flow velocity predicts poor outcome in subarachnoid hemorrhage. *Stroke* 2004; 35: 1873–1878.